An Algorith to Derive Transfer Function Coefficients for an Auditory Filterbank from Experimental Tuning Curves

Thomas Ostermann
Chair of Research Methodology and Statistics in Psychology, Witten/Herdecke University, 58313 Herdecke, Germany

Keywords: Cochlea, Filterbank, Lowpass, Transfer Function.

Abstract: Auditory processing is one of the most complex and fundamental tasks in human psychophysiology. In the past 150 years researchers have tried to understand how sound and especially speech is processed in the human ear. Today, digital auditory filter models and nonlinear active silicon cochlea models are used to simulate cochlear sound processing. This article therefore aims at describing a simple algorithm to derive transfer functions coefficients for an auditory filterbank from tuning curves. Based on the model of the basilar membrane as a cascade of second order lowpass filters, the transfer functions are adopted to experimental data of tuning curves in the cochlea. With basic information on the shape of the travelling waves the presented algorithm is able to derive transfer function coefficients for an auditory filterbank. After the algorithm is explained this article shows how to use it in the presence of experimental data, and gives an application to a an operational amplifier filter circuit using active compensation.

1 INTRODUCTION

Auditory processing is one of the most complex and fundamental tasks in human psychophysiology. In the past 150 years researchers have tried to understand how sound and especially speech is processed in the human ear. While Helmholtz in his book “On the sensations of tone as a physiological basis for the theory of music” proposed a resonance concept (Helmholtz, 1868), his idea was contradicted by Wien (Wien, 1905), who stated that high selectivity and high damping of the ear could anatomically not be realized in the cochlea. On the experimental site, von Bekesy found that frequency-to-place transformation in the cochlea was not caused by resonance but by traveling waves on the basilar membrane (von Zimmermann, 1993; Ostermann et al., 2002). In a variety of experiments on animal ears post mortem von Bekesy measured the displacement of the basilare membrane in a prepared cochlea for tonal stimuli and displayed them as a function of frequency with the maximal displaced normalized as 100% displacement (see Fig. 1 for an original graph from Bekesy, 1944 and Fig. 2 for a schematic drawing of the cochlea).

Mathematical modeling approaches like the transmission-line models Peterson and Bogert (Peterson and Bogert, 1950) or the hydrodynamical model of Ranke (Ranke, 1950) very early proposed the use of electronic filters for simulating cochlea mechanics and finally led to the concept to model the basilar membrane as a cascade of filters.

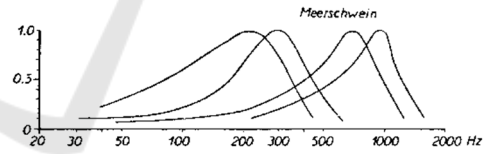

Figure 1: Normalized travelling waves on the basilare membrane of the guinea pig (from Bekesy, 1944).

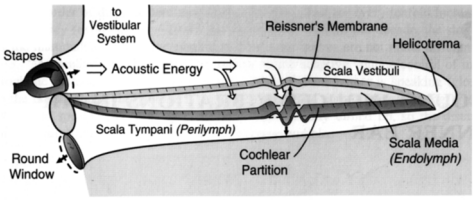

Figure 2: Schematic drawing and inner ear dynamics of the Cochlea (from Wen, 2006).

A non-logartithmic modeling approach for the tuning curves is given in Fig. 3, while Fig. 4 gives values for the renomalization of the travelling waves in Fig 1.

Ostermann, T.
An Algorith to Derive Transfer Function Coefficients for an Auditory Filterbank from Experimental Tuning Curves.
DOI: 10.5220/0005657001940199
In *Proceedings of the 9th International Joint Conference on Biomedical Engineering Systems and Technologies (BIOSTEC 2016) - Volume 5: HEALTHINF*, pages 194-199
ISBN: 978-989-758-170-0
Copyright © 2016 by SCITEPRESS – Science and Technology Publications, Lda. All rights reserved

Several electronical models adopted the idea of a filterbank to model the the cochlea. In 1972 David presented a analogue lowpass filterbank of 64 cascaded 2nd order lowpass filters (David, 1972). A similar model was constructed by Richter in 1977 which in addition contained electronical circuits to simulate activen backcoupling in the basilare membrane (Richter, 1977).

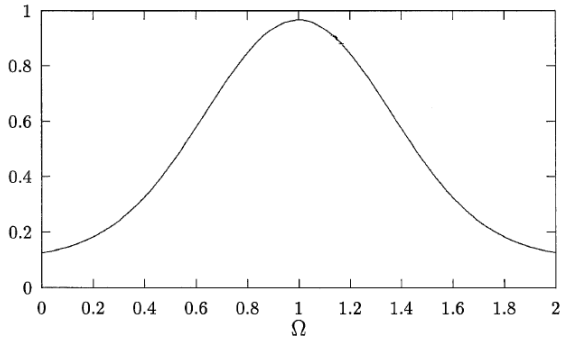

Figure 3: Modeling approach for a normalized tuning curve h(Ω). Ω denotes the normalized frequency with respect to f_{max} (from Ostermann,1995).

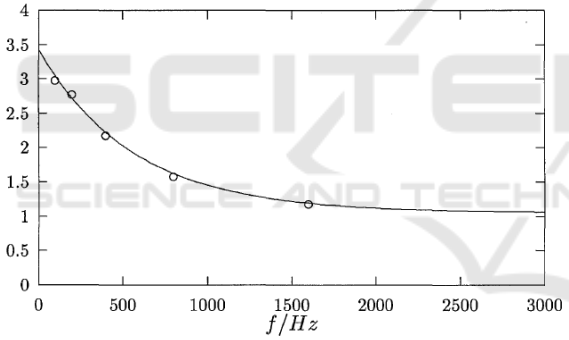

Figure 4: Renomalization *r(f)* of the tuning curves (from Ostermann,1995).

Today, digital auditory filter models have replaced analogue filters and nonlinear active silicon cochlea models are created using very large scale integration (VLSI) to simulate cochlear sound processing (Lyon et al., 2010; Katsiamis and Drakakis, 2011). They are used in a variety of areas, i.e. in the assessment of sound quality (Harlander et al., 2014), for cochlea implants (Cosentino et al., 2014), the recognition and analysis of speech emotion recognition (Aher and Cheeran, 2014).

However the question still remains how to determine the filter coefficients from the basis of tuning curve data such as given in Fig 1.

This article describes therefore aim at describing a simple and straightforward algorithm to derive transfer functions coefficients for a auditory filterbank from tuning curves.

2 MATERIAL AND METHODS

We first define f_{max} as that frequency in which the amplitude of the basilare membrane has its maximum. Then $\Omega = {}^{f}\!/_{f_{\max}}$ denotes the normalized frequency with respect to f_{max}. Keeping in mind the frequency-to-place transformation in the cochlea, every frequency f is mapped to a unique place on the basilare membrane.

Next the transfer function for a lowpass according to (Furth and Andreou, 1995) is defined by

$$H(\Omega) = \frac{a_0 + ia_1\Omega}{b_0 + ib_1\Omega - b_2\Omega^2}$$

and its amplitude given by

$$\begin{aligned} |H(\Omega)| &= \sqrt{\frac{a_0^2 + a_1^2\Omega^2}{\left(b_0 - b_2\Omega^2\right)^2 + b_1^2\Omega^2}} \\ &= \alpha\sqrt{\frac{1+\beta^2\Omega^2}{\left(1-\gamma\Omega^2\right)^2 + \varepsilon^2\Omega^2}} \end{aligned} \quad (1)$$

with $\alpha = \frac{a_0}{b_0}$, $\beta = \frac{a_1}{a_0}$, $\gamma = \frac{b_2}{b_0}$, $\varepsilon = \frac{b_1}{b_0}$.

Let $h(\Omega_N)$ now denote the N^{th} function of the tuning curve given in figure 1 and $r(f_{gN})$ denote the renormalisation function for the peak of the tuning curves (see figures 3 and 4), we can write the N^{th} and $(N+1)^{th}$ renormalized tuning curve as a product of lowpass filters:

$$h(\Omega_N)r(f_{gN}) = \prod_{i=1}^{N}|H(\Omega_i)|$$

$$h(\Omega_{N+1})r(f_{gN+1}) = \prod_{i=1}^{N+1}|H(\Omega_i)|$$

To obtain the transfer function of the $(N+1)^{th}$ lowpass filter, we then get:

$$|H(\Omega_{N+1})| = \frac{h(\Omega_{N+1})r(f_{gN+1})}{h(\Omega_N)r(f_{gN})} \quad (2)$$

From Equation (1) we find that

$$|H(0)| = \alpha = \frac{r(f_{gN+1})}{r(f_{gN})} \quad (3)$$

SCITEPRESS SCIENCE AND TECHNOLOGY PUBLICATIONS

To ease the next calculations and without loss of generality, α is set to 1 in the following calculations.

Next it is required that location and value of the maximum of $|H(\Omega_{N+1})|$ correspond to the respective values of

$$\frac{h(\Omega_{N+1})r(f_{gN+1})}{h(\Omega_N)r(f_{gN})}$$

By calculating the first derivate $|H(\Omega)|'$, and equate it to zero, we get

$$\beta^2 + 2\gamma - \varepsilon^2 - 2\gamma^2\Omega^2 - \beta^2\gamma^4\Omega^4 = 0$$

which leads to

$$\Omega_{\max}^2 = -\frac{1}{\beta^2} + \frac{1}{\gamma\beta^2}\sqrt{(\gamma+\beta^2)^2 - \beta^2\varepsilon^2} \qquad (4)$$

and it follows that

$$\varepsilon^2 = 2\gamma + \beta^2 - 2\gamma^2\Omega_{\max}^2 - \gamma^2\beta^2\Omega_{\max}^4 \qquad (5)$$

Taking into account that $\Omega_{\max}^2 \geq 0$, equation (4) also requires that

$$\frac{1}{\gamma}\sqrt{(\gamma+\beta^2)^2 - \beta^2\varepsilon^2} \geq 1$$

which is equivalent to

$$2\gamma \geq \varepsilon^2 - \beta^2$$

Inserting (5) into (1) leads to

$$\gamma = \sqrt{\frac{|H(\Omega_{\max})|^2 - 1 - \beta^2\Omega_{\max}^2 + \beta^2\Omega_{\max}^2|H(\Omega_{\max})|^2}{\Omega_{\max}^4|H(\Omega_{\max})|^2 + \beta^2\Omega_{\max}^6|H(\Omega_{\max})|^2}} \qquad (6)$$

Finally |H(Ω)| for Ω=1 can be derived from the right side of (2) and thus using (1) we have

$$|H(1)| = \sqrt{\frac{1+\beta^2}{(1-\gamma)^2+\varepsilon^2}}$$

which leads to

$$\beta^2 = |H(1)|^2\left((1-\gamma)^2 + \varepsilon^2\right) \qquad (7)$$

By substituting and solving equations (5) to (7), the remaining parameters can now be obtained. To simplify the equations, we define the following parameters:

$$a = |H(1)|\ b = |H(\Omega_{\max})|,\ c = \Omega_{\max}.$$

With $\Psi(\Omega) := \frac{h(\Omega_{N+1})}{h(\Omega_N)}$ we finally get the algorithm given in table 1:

Table 1: Algorithm to determine the coefficients of the transfer function.

For every N calculate:

$$a = \Psi(1)$$

$$b = \Psi(\Omega_{N+1\max})$$

$$c = \Omega_{N+1\max}$$

$$\beta^2 = \frac{a^2(1-b^2-2c^2-b^2c^4+2b^2c^2)+b^2c^4}{(a^2-b^2)c^4}$$

$$\gamma = \sqrt{\frac{b^2-1-\beta^2c^2-\beta^2b^2c^2}{c^4b^2)+\beta^2c^6b^2}}$$

$$\varepsilon^2 = 2\gamma + \beta^2 - 2\gamma^2c^2 - \gamma^2\beta^2c^4$$

3 RESULTS

The algorithm is now applied to experimental data. Therefore the functions for *h(Ω)* and *r(f)* from Fig. 3 and Fig.4 have to be given explicitly. In (Ostermann, 1995) a nonlinear regression model was applied to the experimental data and found the following equation:

$$h(\Omega) = 0.11 + 0.86 \cdot \exp(-3.76(\Omega-1)^2) \qquad (8)$$

and

$$r(f_g) = 1.052 + 2.388 \cdot \exp(-0.002 \cdot f_g) \qquad (9)$$

Using (8) we get

$$\frac{h(\Omega_{N+1})}{h(\Omega_N)} = \frac{0.11+0.86\cdot\exp(-3.76(\Omega_{N+1}-1)^2)}{0.11+0.86\cdot\exp(-3.76\frac{f_{gN+1}^2}{f_{gN}^2}(\Omega_{N+1}-\frac{f_{gN+1}}{f_{gN}})^2)}$$

A model fit with this algorithm for f_g = 200Hz is shown in Fig. 5.

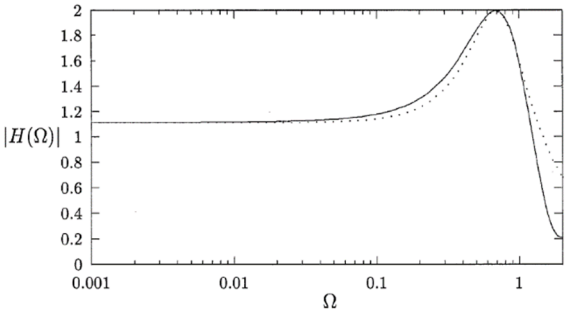

Figure 5: Original curve (solid line) and model fit (dotted line) for f_g=200Hz.

As can be seen the fitting quality is not sufficient in the stopband region of the filter. Therefore, we modified the algorithm given in table 1 with respect to the parameter a:

$$a = \xi \cdot \Psi(1), \text{ with } \xi \in [0,1]$$

For every ξ the parameters β^2, γ and ε^2 are calculated. In addition, the integral

$$\text{int} = \int_0^2 \left[\, | H(\Omega) | - \Psi(1) \right]^2 d\Omega,$$

which defines the area between the two curves in Fig. 5 is numerically minimized and that value of ξ is chosen which minimizes the integral. Table 2 summarizes the results with respect to the cut-off frequency f_g:

Table 2: Parameters of int, ξ, β^2, γ, ε^2 and α for cut-off frequencies f_g between 200 and 3150Hz.

f_g/Hz	int	ξ	β^2	γ	ϵ^2	α
3150	0.00344	0.94	1.68221	1.59015	2.27099	1.00502
2700	0.00300	0.94	1.65778	1.57349	2.29581	1.00988
2320	0.00290	0.94	1.64866	1.56711	2.30454	1.01725
2000	0.00279	0.94	1.63637	1.55841	2.31580	1.02658
1720	0.00286	0.94	1.64544	1.56485	2.30754	1.03865
1480	0.00285	0.94	1.64342	1.56341	2.30942	1.05068
1270	0.00295	0.94	1.65364	1.57060	2.29982	1.06304
1080	0.00349	0.93	1.53558	1.59280	2.17341	1.07669
920	0.00339	0.94	1.68013	1.58876	2.27319	1.08195
770	0.00458	0.92	1.45337	1.62698	2.03462	1.09370
630	0.00668	0.91	1.40044	1.66619	1.88215	1.10363
510	0.00785	0.90	1.31462	1.68127	1.78048	1.10152
400	0.01204	0.88	1.19009	1.71576	1.56432	1.10378
300	0.01933	0.86	1.11328	1.74352	1.33695	1.10314
200	0.04549	0.83	1.12267	1.74275	0.93884	1.11184

To illustrate the results, Fig. 6 shows the original curve and the model fit for the cut-off frequencies 200Hz, 1480Hz and 2700Hz.

The agreement of model fit and empirical data increases with increasing cut off frequency. For a transfer function $H(s)$ with $s=i\Omega$

$$H(s) = \frac{\tilde{a}_0 + \tilde{a}_1 s}{\tilde{b}_0 + \tilde{b}_1 s + s^2}$$

the coefficients β^2, γ, ε^2 and α given in Table 2 can easily be transformed. The respective values are given in table 3.

Now, the coefficients for designing the filters are given and can be applied to filter circuits using i.e. operational amplifiers (OPAMS).

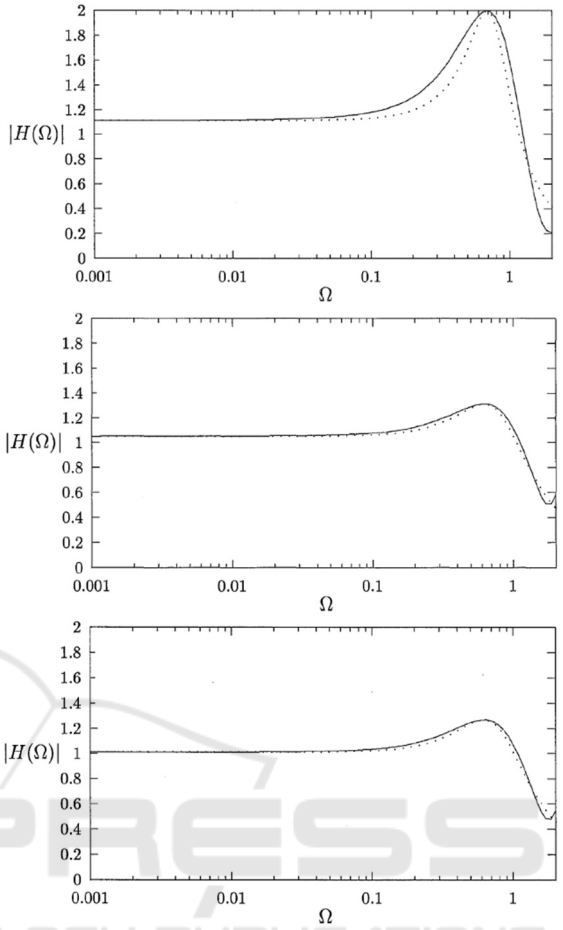

Figure 6: Original curve (solid line) and model fit (dotted line) for f_g=200Hz, 1480Hz and 2700Hz (top to down).

Table 3: Parameters of $\tilde{a}_0, \tilde{a}_1, \tilde{b}_0$ and $\tilde{b}_1$ for cut-off frequencies f_g between 200 and 3150Hz.

f_g/Hz	$\tilde{a}_0$	$\tilde{a}_1$	$\tilde{b}_0$	$\tilde{b}_1$
3150	0.63203	0.81974	0.62887	1.50698
2700	0.64181	0.82636	0.63553	1.51519
2320	0.64912	0.83348	0.63812	1.51807
2000	0.65874	0.84266	0.64168	1.52177
1720	0.66374	0.85141	0.63904	1.51906
1480	0.67204	0.86153	0.63963	1.51968
1270	0.67684	0.87037	0.63670	1.51652
1080	0.67597	0.83766	0.62783	1.47425
920	0.68100	0.88271	0.62942	1.50771
770	0.67223	0.81041	0.61464	1.42640
630	0.66237	0.78385	0.60017	1.37191
510	0.65517	0.75120	0.59479	1.33435
400	0.64332	0.70180	0.58283	1.25073
300	0.63271	0.66758	0.57355	1.15627
200	0.63798	0.67598	0.57381	0.96894

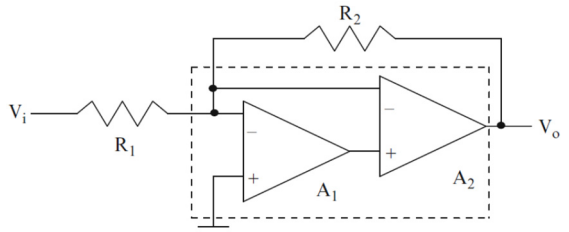

Figure 7: Example of a filter circuit using active compensation from (Mohan, 2013).

The transfer function of this filter is given by

$$H(s) = -\frac{R_2}{R_1}\frac{1+\frac{s}{B_2}}{1+\frac{s}{B_2}+\frac{s^2}{B_1B_2}(1+\frac{R_2}{R_1})}$$

where R_1 and R_2 are the resistor values and B_1 and B_2 denote the unity gain bandwidths of the OPAMS.

4 CONCLUSIONS

Auditory filterbanks to simulate the cochlea have a long history dating back to the 1950th. This article presents an algorithm to derive transfer functions for an auditory filterbank from experimental tuning curves. Based on experimental data, tuning curves were mathematically modelled and after some transformations the coefficients of the transfer function can be determined and be realized either in analogue or digital filters.

Apart from the analysis of sound, such models can also provide useful insights for students in the field of auditory physiology i.e. to simulate patients' hearing loss. Such a system has actually been realized by means of digital filters (Hohenberg et al., 2016).

This approach has also its limitations. It is based on the assumption that tuning curves and frequency-to-place transformation in the cochlea can be modelled by a simple exponential approach. We also assumed that the shape of the tuning curves does not change. However, as Lyon et al., (2010) have pointed out, physiological data show a filter shape asymmetry. Finally this approach only models the passive part of the cochlea. However there is also an active back coupling which is not part of this algorithm and has to be integrated by means of positive feedback loop circuits (Ostermann, 2002; Katsiamis et al., 2009; Elliott and Shera, 2012). Thus, more extensive experimental analysis is needed to validate the proposed algorithm.

However, if data can be modelled like in the present article, this algorithm can be a part of a straight forward approach to establish an auditory filterbank.

ACKNOWLEDGEMENT

I would like to thank Roland Zieke, University of Osnabrück, Germany for his support in this project.

REFERENCES

Aher, P., & Cheeran, A., 2014. Auditory Processing of Speech Signals for Speech Emotion Recognition. *International Journal of Advanced Research in Computer and Communication Engineering, 3(5),* 6790-93.

Cosentino, S., Falk, T. H., McAlpine, D., & Marquardt, T., 2014. Cochlear implant filterbank design and optimization: A simulation study. *IEEE/ACM Transactions on Audio, Speech, and Language Processing*, *22(2)*, 347-353.

David, E., 1972. Elektronisches Analogmodell der Verarbeitung akustischer Information in Organismen, Habil.-Schrift, Universität Erlangen.

Elliott, S. J., Shera, C. A., 2012. The cochlea as a smart structure. *Smart Materials and Structures, 21(6), 064001.*

Furth, P.M., Andreou, A.G., 1995. A Design Framework for Low Power Analog Filter Banks. *IEEE Transactions on Circuits and Systems I: Fundamental Theory and Applications, 42(11),* 966-971.

Harlander, N., Huber, R., & Ewert, S. D., 2014. Sound Quality Assessment Using Auditory Models. *Journal of the Audio Engineering Society*, 62(5), 324-336.

Hohenberg, G., Reiss, G., Ostermann, T., 2016. An interactive digital platform for teaching auditory physiology using two classes of electronic basilare membrane models. *HEALTHINF 2016 - Proceedings of the International Conference on Health Informatics.*

Lyon, R. F., Katsiamis, A. G., Drakakis, E. M., 2010. History and future of auditory filter models. In *Circuits and Systems (ISCAS), Proceedings of 2010 IEEE International Symposium: 3809-3812.*

Katsiamis, A., Drakakis E., Lyon R.F., 2009. A biomimetic, 4,5W, 120+dB, log-domain cochlea channel with ACG. *IEEE Journal of Solid-State Circuits, 44(3),* 1006-1022.

Katsiamis, A., Drakakis E., 2011. Analogue CMOS cochlea systems: A historic retrospective", Biomimetic Based Applications, *InTech, available from http://www.intechopen.com/books/biomimetic based-applications/analogue-cmos-cochlea-systems-a-historicretrospective, 2011.*

Mohan, P. A., 2013. Active RC Filters Using Opamps. In *VLSI Analog Filters. Birkhäuser Boston: 13-146.*

Ostermann, T., 1995. Parameterbestimmung zur Modellierung der Schallwirkung in der Cochlea mittels elektronischer Bauteile. *Diplomarbeit im Fachbereich Mathematik der University of Osnabrück.*

Ostermann, T., Zielke, R., David, E., 2002. Eine mathematisch-technische Modellierung von passiven und aktiven Schwingungsformen der Basilarmembran. *Biomedical Engineering, 47(1-2), 14-19.*

Peterson, L., Bogert, B., 1950. A dynamical theory of the cochlea. *JASA 22, 369-381.*

Ranke, O.F., 1950. Hydrodynamik der Schnecken-flüssigkeit, *Zs. f. Biol. 103, 409-434.*

Richter, A.,1976. Ein Funktionsmodell zur Beschreibung der amplitudenabhängigen selektiven Eigenschaften des Gehörs. *Dissertation, TU München.*

Von Békésy, G., 1944. Über die mechanische Frequenzanalyse in der Schnecke verschiedener Tiere. *Akust. Z., 9, 3-11.*

Von Helmholtz, H. , 1865. Die Lehre von den Tonempfindungen als physiologische Grundlage für die Theorie der Musik. Vieweg, Braunschweig.

Wen, B., 2006. Modeling the nonlinear active cochlea. Doctoral dissertation, University of Pennsylvania.

Wien, M., 1905. Ein Bedenken gegen die Helmholtzsche Resonanztheorie des Hörens. *In: Festschrift Adolph Wüllner gewidmet zum 70. Geburtstage. Teubner, Leipzig: 28–35.*

Zimmermann, P., 1993. Entwicklungslinien der Hörtheorie. *NTM International Journal of History & Ethics of Natural Sciences, Technology & Medicine, 1(1), 19-36.*

SCITEPRESS
SCIENCE AND TECHNOLOGY PUBLICATIONS